Small-angle neutron scattering of nanocrystalline gadolinium and holmium with random

paramagnetic susceptibility

Small-angle neutron scattering of nanocrystalline gadolinium and holmium with random paramagnetic susceptibility

Frank Döbrich[1,4]**, Jens-Peter Bick**[1]**, Rainer Birringer**[2]**, Matthias Wolff**[2]**, Joachim Kohlbrecher**[3] **and Andreas Michels**[1]

[1] Physics and Materials Science Research Unit, University of Luxembourg, 162A Avenue de la Faïencerie, L-1511 Luxembourg, Grand Duchy of Luxembourg
[2] Experimentalphysik, Universität des Saarlandes, D-66041 Saarbrücken, Germany
[3] Paul Scherrer Institut, CH-5232 Villigen PSI, Switzerland

E-mail: frank.doebrich@uni-saarland.de and andreas.michels@uni.lu

CrossMark

Abstract

A neutron study of nanocrystalline terbium (Balaji G *et al* 2008 *Phys. Rev. Lett.* **100** 227202) has shown that the randomly oriented anisotropy of the paramagnetic susceptibility tensor may lead to strongly correlated nanoscale spin disorder in the paramagnetic state which can be probed very effectively by magnetic small-angle neutron scattering (SANS). In principle, this scenario is also applicable to other rare-earth metals and the size of the effect is expected to scale with the strength of the anisotropy in the paramagnetic state. Here, we report SANS results (in the paramagnetic state) on nanocrystalline inert-gas condensed samples of Gd and Ho, which represent the cases of low and high anisotropy, respectively.

Keywords: magnetic materials, rare-earth metals, small-angle neutron scattering, magnetic anisotropy

(Some figures may appear in colour only in the online journal)

1. Introduction

As a consequence of the large volume fraction of grain boundaries, typical average crystallite sizes between 10–50 nm and a random orientation of the crystallographic axes, nanocrystalline *inert-gas condensed* materials are excellent model systems for investigating the impact of internal interfaces and reduced structural length scales on the magnetic properties of solids [1]. In recent years, the eminent potential of the magnetic small-angle neutron scattering (SANS) technique for studying the magnetic microstructure of nanocrystalline ferromagnetic materials has been demonstrated [2]. In particular, using magnetic SANS, characteristic parameters such as the correlation length of the spin misalignment, the exchange-stiffness constant, or the mean-square internal magnetostatic stray field have been retrieved.

Due to the position-dependent Ruderman–Kittel–Kasuya–Yosida exchange interaction between the highly localized magnetic moments, the magnetism of the rare-earth metals is particularly prone to structural disorder [3]. Furthermore, the random jump in the direction of the magnetocrystalline anisotropy axes across grain boundaries is expected to be particularly relevant in the rare-earth metals with an orbital angular momentum $L \neq 0$. Up to date, only two SANS studies on nanocrystalline rare-earth ferromagnets exist: on Tb ($L = S = 3$) as a representative of a material with strong magnetocrystalline anisotropy [4] and on Gd ($L = 0$, $S = 7/2$) (using the low-capturing isotope ^{160}Gd) with a comparatively low anisotropy [5] (S: spin angular momentum). Both investigations demonstrate a strong impact of the nanoscale microstructure on the *ferromagnetic* spin structure.

[4] Present address: Patentverwertungsagentur der saarländischen Hochschulen (PVA), Universität des Saarlandes, Wissens- und Technologietransfer GmbH, Starterzentrum, Gebäude A1 1, D-66123 Saarbrücken, Germany.
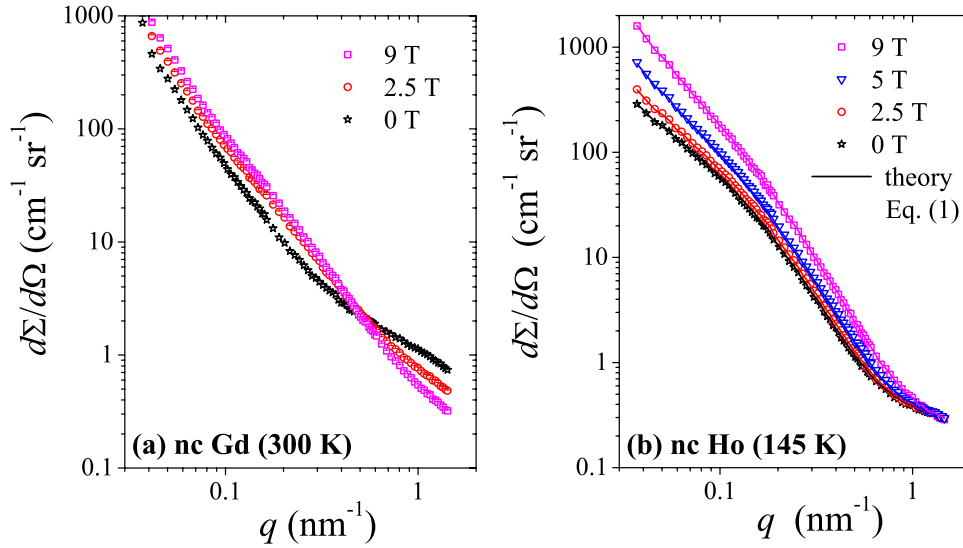
Figure 1. Azimuthally-averaged unpolarized SANS intensity of (*a*) nanocrystalline ^{160}Gd at $T = 300$ K and (*b*) nanocrystalline Ho at $T = 145$ K for applied-field values as indicated (log–log scale); additional neutron data at intermediate field values are not displayed for clarity. Error bars of the experimental data are of the order of the size of the data points. Solid lines in (*b*) are theoretical predictions by equation (1) (see text).

Moreover, the recent study of the *paramagnetic* SANS from nanocrystalline Tb reported in [6] has revealed a (somewhat counterintuitive) *increase* of the scattering intensity by almost two orders of magnitude with increasing field (from 0–5 T) at low momentum transfers q, whereas the scattering was found to decrease at high q-values. The latter was ascribed to the suppression of local paramagnetic spin fluctuations. Consequently, a rather unusual crossover of the scattering curves at different fields was observed. A quantitative explanation for the increase of the scattering cross section at low q is based on the well-known anisotropy of the paramagnetic susceptibility tensor of Tb [7]. In particular, for the nanocrystalline material, the random orientation of the crystallographic axes of the individual grains gives rise to a highly nonuniform magnetic response on the nanoscale. In other words, in these samples the scattering contrast between neighboring grains (and thus the total scattering cross section) is strongly increased with the field, in contrast to the usual suppression of magnetic nanoscale disorder, which is commonly associated with a decrease of the SANS signal [2].

An important result of the model given in [6] is the quadratic relation of the magnetic SANS cross section to the (internal) applied magnetic field H_i, in agreement with the experimental Tb data. Specifically, for unpolarized neutrons, the azimuthally-averaged differential SANS cross section $\frac{\mathrm{d}\Sigma}{\mathrm{d}\Omega}$ (in the paramagnetic temperature regime) can be expressed as

$$\frac{\mathrm{d}\Sigma}{\mathrm{d}\Omega}(q, H_i) = \frac{\mathrm{d}\Sigma_{\mathrm{nuc}}}{\mathrm{d}\Omega}(q) + S_{\mathrm{mag}}(q)\, H_i^2, \qquad (1)$$

where q is the scattering vector, $\frac{\mathrm{d}\Sigma_{\mathrm{nuc}}}{\mathrm{d}\Omega}$ represents the nuclear scattering cross section and S_{mag} denotes the magnetic scattering function, which is related to the size and shape of the grains as well as to the main-axis entries of the susceptibility tensor (see equation (3) in [6]).

It is the purpose of this study to further investigate the predictions of equation (1) for the case of a low-anisotropy

rare-earth metal (Gd) and for Ho ($L = 6$, $S = 2$), which (similar to Tb) exhibits highly anisotropic magnetic properties.

2. Experimental

Synthesis of disk-shaped nanocrystalline Gd and Ho samples (diameter: 8 mm; thickness: $\sim$500 μm) was carried out by the inert-gas condensation technique, as described in detail in [4, 5, 8]; the Gd samples for the SANS experiments were prepared by employing the low neutron-capturing isotope ^{160}Gd (enrichment: 98.6%) as a starting material in the evaporation process. The average crystallite sizes of the as-prepared nanocrystalline samples were determined by analysis of wide-angle x-ray diffraction data and found to be $D = 21 \pm 6$ nm (Gd) and $D = 51 \pm 7$ nm (Ho). The SANS experiments were performed at the SANS 1 instrument at the Paul Scherrer Institut, Villigen, Switzerland, using unpolarized neutrons with a mean wavelength of $\lambda = 6.0$ Å and a wavelength broadening of $\Delta\lambda/\lambda = 10\%$ (FWHM) [9]. A cryomagnet provided control of the external magnetic field ($\mu_0 H_{\mathrm{max}} = 11$ T) and temperature; the magnetic field **H** was applied perpendicular to the wave vector of the incoming neutron beam. The q-range from $\sim$0.04–1.5 nm^{-1} was covered with three sample-to-detector distances. The neutron raw data were corrected in the usual way for background scattering, transmission, detector efficiency, detector dead time and solid-angle distortion.

3. Results and discussion

Figure 1(*a*) displays the azimuthally-averaged SANS data obtained from the nanocrystalline ^{160}Gd sample at $T = 300$ K, while figure 1(*b*) shows the corresponding data for nanocrystalline Ho at $T = 145$ K. When increasing the field from zero to 9 T, the SANS signal of Gd increases by a factor of about 2 at the lowest momentum transfers (i.e. $q \cong 0.04$ nm^{-1}), whereas at $q \cong 1.5$ nm^{-1} a decrease by a
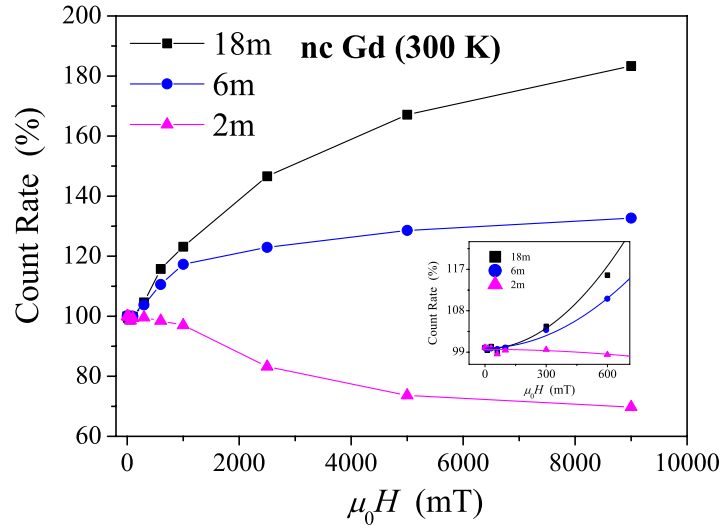
Figure 2. Total detector count rate (normalized to the count rate at zero field) for nanocrystalline ^{160}Gd at $T = 300$ K as a function of the applied magnetic field H at sample-to-detector distances as indicated (18 m corresponding to low q in figure 1(*a*)) (solid lines are guides to the eyes). Insert: low-field regime up to 600 mT. Solid lines represent a fit to equation (1).

factor of 0.4 is found; note that some increase is already visible below 1 T at low and intermediate q. For Ho, it is seen that the SANS intensity increases with the applied field over the *entire* q-range, the maximum effect being found at the lowest q with a factor of approximately 5.4; field values up to 1 T do not induce a significant change in the signal.

The solid lines in figure 1(*b*) represent the prediction by equation (1). For this purpose, the experimental $\frac{d\Sigma}{d\Omega}$ were plotted at each discrete q versus the values of the applied magnetic field. Since $\frac{d\Sigma}{d\Omega}$ is linear in H_i^2 (compare equation (1)), a weighted straight-line fit then provides the values of $\frac{d\Sigma_{nuc}}{d\Omega}$ and S_{mag} at the particular q (see figure 3 below). The values of the theoretical cross sections computed in this way are connected by solid lines in figure 1(*b*). For Ho, we find an excellent agreement between the data and equation (1) over the whole (q, H_i)-range, whereas for Gd the agreement is quantitative only up to fields of ∼0.6 T. This can be seen in figure 2, where the field dependence of the total detector counts of Gd at three different sample-to-detector distances is shown. For field values up to 0.6 T and at intermediate and low q, we find a quadratic increase according to equation (1) (see insert in figure 2), while at higher fields the signal shows a Langevin-like behavior. At high q, the intensity is slightly suppressed with increasing field, which may be attributed to the presence of scattering from critical spin fluctuations [6].

Although for the case of nanocrystalline Gd it is not necessarily expected to see the described effect due to a vanishing difference between the paramagnetic Curie temperature parallel and perpendicular to the hexagonal *c*-direction [7, 10], $\theta_{\parallel} = \theta_{\perp} = 317 \pm 3$ K, the properties of Gd near the Curie point $T_C \cong 293$ K [11] may help to understand the situation in this material. In particular, Gd shows a rather broad Curie transition, strong deviations from Curie–Weiss behavior near T_C (θ was obtained by extrapolation from temperatures above 400 K [10]) and a nonvanishing anisotropy in the paramagnetic regime up to about 340 K [12]. These properties are in line with the observations reported here, i.e. scattering from critical spin fluctuations and due to

random paramagnetic susceptibility, as well as an approach-to-saturation behavior at higher fields. Note also that for a mean grain size of $D = 21$ nm, a reduced Curie temperature of about 285 K is expected [13]. Furthermore, results from a SANS study in the ferromagnetic temperature range showed that in nanocrystalline Gd the grain boundaries are associated with strong nanoscale spin disorder [5]. Grain-boundary effects may also provide a major contribution to the magnetic-field response observed in the paramagnetic regime. However, since grain boundaries are presumably coupled to fluctuations in the paramagnetic susceptibility on rather short real-space length scales, i.e. only a few nanometers, the corresponding magnetic scattering can be expected at the largest q-values. Thus, if present, the signature of the grain boundaries is likely to be covered by critical scattering in the current data for the case of Gd.

The Ho data were measured at 145 K, well above both $\theta_{\parallel} = 73$ K and $\theta_{\perp} = 88$ K as well as the antiferromagnetic Néel Temperature $T_N = 132$ K [7]. Accordingly, we find strong field-induced scattering predominantly at the higher fields and a very good agreement with the model proposed in [6]. No saturation effects are seen in the Ho data, although the SANS measurements were conducted up to 9 T.[5]

Figures 3(*a*) and (*b*) display, respectively, the fit results for $\frac{d\Sigma_{nuc}}{d\Omega}$ and S_{mag} for Gd at $T = 300$ K and for Ho at $T = 145$ K. Integration of the S_{mag}-data, according to

$$Q_p = \frac{45\mu_0^2}{13\pi^2 b_H^2} \int_0^\infty S_{mag} q^2 \, dq = (\chi_{11} - \chi_{33})^2, \qquad (2)$$

yields a partial invariant Q_p of the azimuthally-averaged magnetic scattering cross section (equation (4) in [6]) ($b_H =$

---

[5] This is in contrast to nanocrystalline Tb [6], where the results indicate the onset of saturation already at 5 T, in spite of the paramagnetic anisotropy of Tb being considerably larger than that of Ho. The latter observation may be attributed to the fact that the studied temperature range of 240–280 K is comparatively close to the larger of the two paramagnetic Curie temperatures $\theta_{\parallel} = 195$ K and $\theta_{\perp} = 239$ K of Tb [7].
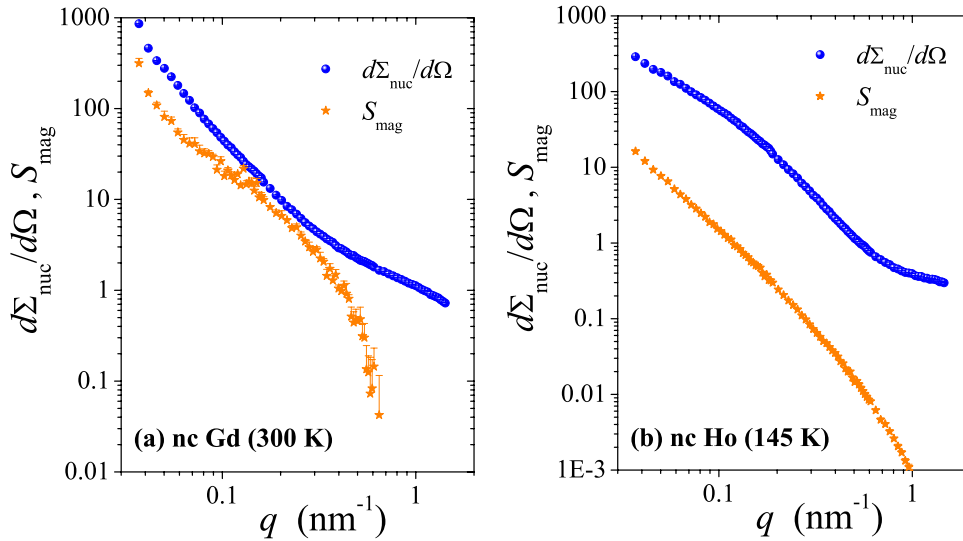
Figure 3. $\frac{d\Sigma_{nuc}}{d\Omega}$ and S_{mag} (in units of $cm^{-1}\,sr^{-1}\,T^{-2}$) of nanocrystalline Gd at $T = 300\,K$ (*a*) and of nanocrystalline Ho at $T = 145\,K$ (*b*) as obtained from the fit of the data shown in figure 1 to equation (1) (log–log scale).

$2.91 \times 10^8\,A^{-1}\,m^{-1}$); Q_p is related to a deviatoric component, $(\chi_{11} - \chi_{33})^2$, of the susceptibilty tensor, where χ_{11} and χ_{33} denote, respectively, the susceptibility along the *a*-axis and *c*-axis of the hcp lattice. When the integration in equation (2) is carried out, we obtain a lower bound for Q_p due to the limited range of experimental scattering vectors ($q_{min} \leqslant q \leqslant q_{max}$).

The resulting value for Ho, $\sqrt{Q_p} \cong 0.060$, compares reasonably with the value of $|\chi_{11} - \chi_{33}| \cong 0.046$ estimated from single-crystal magnetization measurements [14]. Note that the theory behind equation (1) neglects terms of local demagnetizing field and magnetoelastic coupling, which may result in a reduced value of Q_p [6]. Furthermore, our results for nanocrystalline Ho do not provide evidence for grain-boundary-induced effects, as can be seen e.g. from the fact that S_{mag} takes on very low values for *q*-values $>1\,nm^{-1}$ (see figure 3(*b*)). While this does not necessarily imply that grain boundaries have no relevance for the paramagnetic properties of nanocrystalline Ho, we note that the comparatively large crystallite size of 51 nm of the present Ho sample is associated with a volume fraction of grain boundaries of only about 8% [5].

The results for S_{mag} of nanocrystalline Gd (figure 3(*a*)) indicate that the random paramagnetic susceptibility of the individual grains leads to significant correlated nanoscale spin disorder at 300 K and moderate fields in accordance with the model proposed in [6]. From equation (2), a value of $\sqrt{Q_p} \cong 0.27$ can be derived. Note that for $q > 0.5\,nm^{-1}$, S_{mag} could not be evaluated from the present data due to critical scattering. Since $\sqrt{Q_p}$ compares directly with the difference $|\chi_{11} - \chi_{33}|$ and since Gd is known to exhibit by far the lowest magnetocrystalline anisotropy among the heavy rare-earth metals, one may expect to obtain a much lower $\sqrt{Q_p}$-value (for Gd) than for nanocrystalline Ho. However, the experimental temperature value of 300 K differs only by about 15 K from the Curie temperature of nanocrystalline Gd (with $D = 21\,nm$) [13], whereas for the Ho data there is a difference of more than 55 K to $\theta_\perp$, leading to comparatively

low susceptibility values ($\chi \propto (T-\theta)^{-1}$) and, thus, to a small value of $|\chi_{11} - \chi_{33}|$.

The observation of a finite magnetic anisotropy of the susceptibility tensor of Gd in the paramagnetic state may be surprising in view of the fact that the orbital angular momentum of the Gd^{3+}-ion vanishes. This finding indeed addresses fundamental aspects regarding the origin of magnetic anisotropy of Gd metal, which has recently been investigated in the ferromagnetic temperature regime by means of first-principles density functional theory [15]. The authors of [15] have suggested a mechanism for the magnetic anisotropy energy involving (besides dipolar anisotropy) the spin-orbit interaction of the conduction electrons. In this respect, it would be of interest to investigate in detail the origin of the observed magnetic anisotropy of nanocrystalline Gd in the paramagnetic temperature regime.

4. Conclusion

In conclusion, we have performed magnetic-field-dependent SANS measurements on nanocrystalline Gd and Ho in the paramagnetic temperature regime. Our data analysis indicates that, when a magnetic field is applied, random paramagnetic susceptibility leads to strong correlated nanoscale spin disorder in these materials. Equation (1), which predicts $\frac{d\Sigma}{d\Omega} \propto H_i^2$ at low *q*, provides an excellent description of the field-dependent correlations in strongly anisotropic Ho, while for Gd its applicability is limited to fields below about 0.6 T, presumably due to low anisotropy and/or the close proximity to the Curie temperature. However, in view of the pure *S*-state nature of the Gd^{3+}-ion, it appears to be surprising to find a significant nonzero anisotropy of the susceptibility tensor from the neutron data. Future experiments will address the temperature, grain size and, in particular, the polarization dependence of the paramagnetic SANS in order to determine the temperature dependence of the anisotropy parameters and to investigate the role of the grain boundaries for the paramagnetic state of nanocrystalline rare-earth metals.

Acknowledgments

References

[1] Gleiter H 1989 *Prog. Mater. Sci.* **33** 223
[2] Michels A 2014 *J. Phys.: Condens. Matter* **26** 383201
[3] Michels A *et al* 2011 *Phys. Rev.* B **83** 224415
[4] Weissmüller J, Michels A, Michels D, Wiedenmann A, Krill C E III, Sauer H M and Birringer R 2004 *Phys. Rev.* B **69** 054402
[5] Döbrich F, Kohlbrecher J, Sharp M, Eckerlebe H, Birringer R and Michels A 2012 *Phys. Rev.* B **85** 094411
[6] Balaji G, Ghosh S, Döbrich F, Eckerlebe H and Weissmüller J 2008 *Phys. Rev. Lett.* **100** 227202
[7] Legvold S 1980 *Ferromagnetic Materials* vol 1, ed E P Wohlfarth (Amsterdam: North-Holland) pp 183–295
[8] Michels D, Krill C E III and Birringer R 2002 *J. Magn. Magn. Mater.* **250** 203
[9] Kohlbrecher J and Wagner W 2000 *J. Appl. Crystallogr.* **33** 804
[10] Nigh H E, Legvold S and Spedding F H 1963 *Phys. Rev.* **132** 1092
[11] Srinath S and Kaul S N 1999 *Phys. Rev.* B **60** 12166
[12] Graham C D Jr 1963 *J. Appl. Phys.* **34** 1341
[13] Ferdinand A, Probst A C, Michels A, Birringer R and Kaul S N 2014 *J. Phys.: Condens. Matter* **26** 056003
[14] Strandburg D L, Legvold S and Spedding F H 1962 *Phys. Rev.* **127** 2046
[15] Colarieti-Tosti M, Simak S I, Ahuja R, Nordström L, Eriksson O, Åberg D, Edvardsson S and Brooks M S S 2003 *Phys. Rev. Lett.* **91** 157201